Tetrodotoxin-blockable calcium currents in rat ventricular myocytes; a third type of cardiac cell sodium current

R. Aggarwal*, S. R. Shorofsky*, L. Goldman†‡ and C. W. Balke*†‡

*Departments of * Medicine and † Physiology, School of Medicine, University of Maryland, 660 West Redwood Street, Baltimore, MD 21201, USA*

1. Whole-cell patch clamp currents from freshly isolated adult rat ventricular cells, recorded in external Ca^{2+} (Ca_o^{2+}) but no external Na^+ (Na_o^+), displayed two inward current components: a smaller component that activated over more negative potentials and a larger component (L-type Ca^{2+} current) that activated at more positive potentials. The smaller component was not generated by Ca^{2+} channels. It was insensitive to 50 μM Ni^{2+} and 10 μM La^{3+}, but suppressed by 10 μM tetrodotoxin (TTX). We refer to this component as $I_{Ca(TTX)}$.

2. The conductance–voltage, $g(V)$, relation in Ca_o^{2+} only was well described by a single Boltzmann function (half-maximum potential, $V_{½}$, of −44·5; slope factor, k, of −4·49 mV, means of 3 cells). $g(V)$ in Ca_o^{2+} plus Na_o^+ was better described as the sum of two Boltzmann functions, one nearly identical to that in Ca_o^{2+} only (mean $V_{½}$ of −45·1 and k of −3·90 mV), and one clearly distinct (mean $V_{½}$ of −35·6 and k of −2·31 mV). Mean maximum conductance for $I_{Ca(TTX)}$ channels increased 23·7% on adding 1 mM Na_o^+ to 3 mM Ca_o^{2+}. $I_{Ca(TTX)}$ channels are permeable to Na^+ ions, insensitive to Ni^{2+} and La^{3+} and blocked by TTX. They are Na^+ channels.

3. $I_{Ca(TTX)}$ channels are distinct from classical cardiac Na^+ channels. They activate and inactivate over a more negative range of potentials and have a slower time constant of inactivation than the classical Na^+ channels. They are also distinct from yet another rat ventricular Na^+ current component characterized by a much higher TTX sensitivity and by a persistent, non-fast-inactivating fraction. That $I_{Ca(TTX)}$ channels activate over a more negative range of potentials than classical cardiac Na^+ channels suggests that they may be critical for triggering the ventricular action potential and so of importance for cardiac arrhythmias.

Tetrodotoxin (TTX)-blockable calcium currents, $I_{Ca(TTX)}$, have been reported in human atrial (Lemaire, Piot, Seguin, Nargeot & Richard, 1995) and guinea-pig ventricular (Leblanc, Chartier, Martin & Cole, 1996) cells, and in neural preparations (Meves & Vogel, 1973; Akaike & Takahashi, 1992). We describe here an $I_{Ca(TTX)}$ in rat ventricular cells. We find the channels producing this current are permeable to both Na^+ and Ca^{2+}, but are separate from those generating both the L- or T-type Ca^{2+} current, the classical cardiac Na^+ current, I_{Na}, and an additional I_{Na} component reported in rat ventricular cells (Saint, Ju & Gage, 1992). Our (and other) results indicate that $I_{Ca(TTX)}$ is generated by Na^+ channels. We show here that $I_{Ca(TTX)}$ is functionally distinct from all other characterized Na^+ current components in rat ventricular myocytes. It is a new, previously undescribed ventricular Na^+ current component. The channels generating $I_{Ca(TTX)}$ constitute, then, either a differentially regulated, post-translationally modified, or novel cardiac Na^+ channel isoform.

These channels are activated over a more negative potential range than are the classical cardiac Na^+ channels and should, therefore, play a critical role in depolarizing the membrane potential to action potential threshold. Hence, they may be of some importance in cardiac arrhythmias. A variety of nerve, muscle, cardiac and other cell types have been shown to have more than one kind of Na^+ channel (see Discussion). For cardiac cells, clear evidence for more than one Na^+ component has been presented for rat ventricular myocytes (Cachelin, DePeyer, Kokubun & Reuter, 1983; Kunze, Lacerda, Wilson & Brown, 1985; Saint *et al.* 1992), chick ventricular myocytes (Ten Eick, Yeh & Matsuki, 1984), canine cardiac Purkinje fibres (Scanley & Fozzard, 1987), human atrial cells (Sakakibara *et al.* 1992; Lemaire *et al.* 1995), rabbit Purkinje and ventricular cells (Zilberter,

‡ To whom correspondence should be addressed.

Starmer, Starobin & Grant, 1994) and guinea-pig ventricular myocytes (Leblanc *et al.* 1996). This widespread occurrence suggests that more than one Na^+ current component may be a feature of some general importance for cardiac electrophysiology and rhythmicity.

Preliminary reports of some of these results have been made (Thomas, Balke & Shorofsky, 1995; Goldman, Aggarwal, Shorofsky & Balke, 1997).

METHODS

Preparation

Two-month-old Sprague–Dawley rats (200–300 g) were anaesthetized with sodium pentobarbitone (170 mg kg^{-1} injected I.P.). The hearts were removed from the animals via mid-line thoracotomy, and single ventricular cells were obtained by an enzymatic dispersion technique described in detail previously (Balke & Wier, 1992). The cells were studied within 8 h of isolation. Small aliquots of freshly isolated myocytes were placed in a perfusion chamber mounted on the stage of an inverted microscope (Nikon Diaphot). The chamber was specially designed to rapidly change the solution bathing the cells. All experiments were performed at room temperature (21–23 °C).

Electrical recording

Membrane currents were recorded using the whole-cell configuration of the patch clamp technique. Glass suction pipettes were fabricated from borosilicate capillary glass using a Flaming–Brown type micropipette puller (model P-87; Sutter Instruments). When filled with the pipette solution (see below) the electrodes had resistances of 2–3 MΩ. Potential differences between the bath and pipette solutions were compensated prior to patch formation. After formation of a high resistance seal (> 5 GΩ), gentle suction was applied to rupture the cell membrane allowing access to the cell interior.

Whole-cell currents were recorded using an Axopatch 200A amplifier (Axon Instruments). Voltage clamp protocols were generated and whole-cell currents recorded using a 12 bit, A/D board (Labmaster, Scientific Solutions, Solon, OH, USA), under computer control (Dell 486-33 MHz PC using Fastlab software; Indec Systems, Sunnyvale, CA, USA). Series resistance compensation was used in all experiments. Currents were filtered at 2 kHz and digitized at 5–20 kHz. All data were stored on hard disk for subsequent analysis.

Leak and capacity components were measured by application of a 10 mV hyperpolarizing voltage step from a holding potential of −80 mV. The area under the capacity transient was integrated and used to calculate cell capacitance for each experiment. The average cell capacitance was 141 ± 14 pF. All experiments were performed from a holding potential of −100 mV.

Solutions

Cells were continuously superfused (rate of 2–3 ml min^{-1}) with a salt-containing solution of the following composition (mM): 135 NaCl, 10 glucose, 10 Hepes, 10 CsCl, 1 $MgCl_2$, 1 $CaCl_2$ (pH

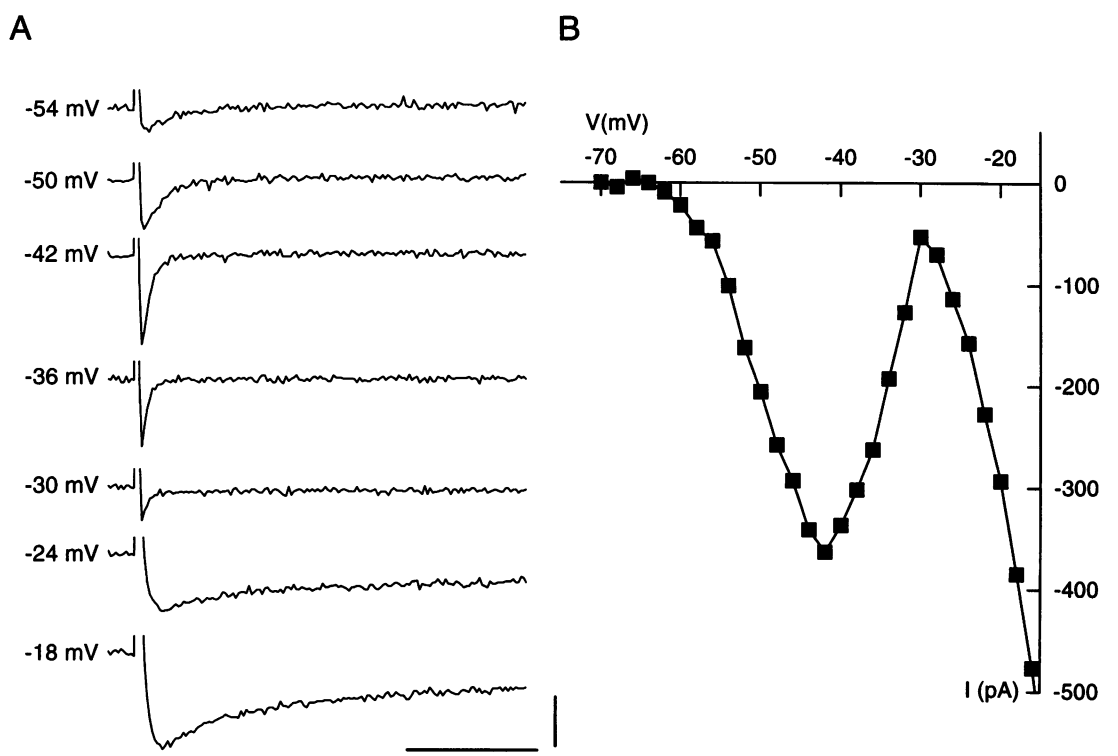

Figure 1. Current records and current–voltage relation in the absence of external Na^+ but presence of 1 mM Ca_o^{2+}

A, whole-cell patch clamp currents, all from the same cell, recorded at each of the indicated potentials. Holding potential was −100 mV. Scale bars represent 200 pA and 50 ms. *B*, peak current–voltage relation for this same cell. Two inward current components are evident.

adjusted to 7·3 with CsOH). The electrode-filling solution contained (mM): 120 glutamic acid, 120 CsOH, 10 Hepes, 0·33 $MgCl_2$, 20 tetraethylammonium chloride (TEA-Cl), 4 Mg-ATP, and 5 EGTA (pH adjusted to 7·3 with CsOH). A 2–3 min equilibration period was allowed after seal formation and establishment of whole-cell recording configuration, and the cells were then superfused with a bathing solution containing (mM): 140 TEA-Cl, 10 glucose, 10 Hepes, 10 CsCl, 1 $MgCl_2$ (pH adjusted to 7·3 with CsOH) and either 1–2 mM Na^+ and/or 0·5–5 mM Ca^{2+} as indicated. A few experiments were done with 140 mM CsCl replacing the TEA-Cl with no obvious effects on the results. Data acquisition began 5 min after initiating superfusion with this new bathing solution.

RESULTS

Ventricular cells display two inward calcium current components

In the presence of 1 mM Ca_o^{2+}, and no Na_o^+, rat ventricular cells show two inward current components. Figure 1*A* presents whole-cell patch clamp records from one cell. Transient inward currents recorded on steps from −100 mV to each of the indicated potentials are shown. With increasingly positive steps in potential, inward current amplitude first increased (records at −54, −50 and −42 mV) and then decreased (records at −36 and −30 mV). However, even more positive voltage steps to −24 and −18 mV evoked currents whose amplitudes again increased, now with slower kinetics. The peak current–voltage relation from −70 to −16 mV for this same cell is shown in Fig. 1*B*. Peak inward current increased from −62 to −42 mV, then decreased to a local minimum at −30 mV, and increased again, thus defining two inward current components.

Two inward current components were seen, under these experimental conditions, in every cell studied (more than 100 cells). Figure 2 shows the mean peak current–voltage relation pooled from the twenty cells for which data were available over an extended range of potentials in 1 mM Ca_o^{2+}. The inward component that activated over more positive potentials reached a maximum at 0–10 mV before declining.

Although the two inward current components approach reversal at very different potentials, they are both carried by Ca^{2+} ions. Figure 3 presents three current–voltage relations from the same cell. In the presence of 1 mM Ca_o^{2+} but no Na_o^+, the usual two inward current components are seen (○). Replacing the bathing medium with a nominally Ca^{2+}-free but otherwise identical solution abolished both inward current components (□) which were restored on return to the 1 mM Ca_o^{2+} external solution (△). Identical results were obtained in four additional cells. Both inward components are Ca^{2+} current components. The very different apparent reversal potentials suggests that the channels generating these two components have different selectivities for Ca^{2+} over any residual permeant internal ions. The larger inward component activated over more positive potentials is generated by L-type Ca^{2+} channels (Fox, Nowycky & Tsien, 1987).

The Ca^{2+} current component activated at more negative potentials does not flow through Ca^{2+} channels

Ni^{2+} is a blocker of Ca^{2+} channels (Mitchell, Powell, Terrar & Twist, 1983). Figure 4*A* shows three current–voltage relations from a single cell, all in the presence of Ca_o^{2+} but no Na_o^+. Adding Ni^{2+} at 50 μM (□) sharply reduced the L-type current seen before exposure to Ni^{2+} (○), but had no effect on the smaller, more negative voltage range-activated component. On removal of Ni^{2+} (△), the L-type current partially recovered. Similar results were obtained in four additional cells.

Another blocker of Ca^{2+} channels is La^{3+} (Wendt-Gallitelli & Isenberg, 1985). Figure 4*B* shows that La^{3+}, too, has no effect on the smaller, more negative voltage-activated component. Three current–voltage relations from a single cell, all in Ca_o^{2+} but no Na_o^+, are shown. La^{3+} at 10 μM (□) fully abolished the L-type current seen before exposure to La^{3+} (○), but had no effect on the other component. On removal of La^{3+} (△) the L-type current partially recovered.

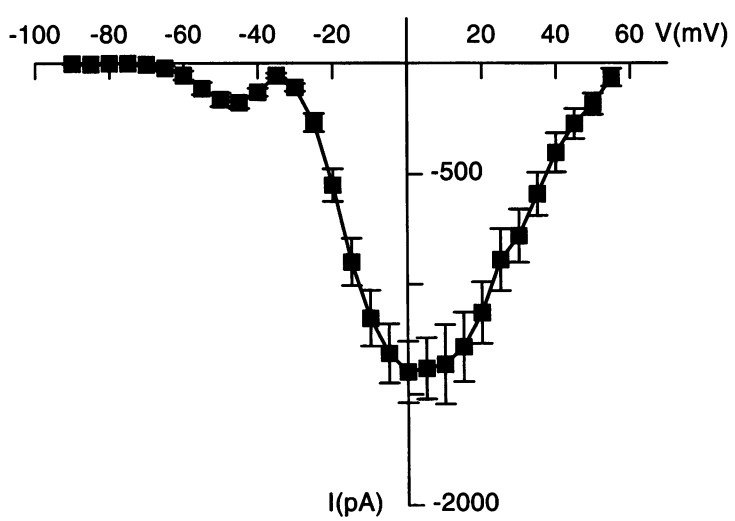

Figure 2. Collected peak current–voltage data in 1 mM Ca_o^{2+} and 0 Na_o^+

Values pooled from 20 cells. Holding potential was always −100 mV. Filled squares are means and error bars indicate S.D.

Similar results were obtained in two additional cells. Hence two known blockers of Ca^{2+} channels have no effect on this smaller, more negative voltage-activated inward current component.

This smaller inward current component is blocked, however, by the Na^+ channel agent TTX. Figure 4*C* shows current–voltage relations from a single cell, again in Ca_o^{2+} but no Na_o^+, in the presence (□) and absence (○, △) of 10 μM TTX. Before exposure to TTX (○) the usual two inward current components are evident. In the presence of 10 μM TTX the smaller, more negative potential range-activated component was blocked completely while the L-type current was unaffected. On removal of TTX, the smaller component returned to its previous values (△). The smaller inward current component was always blocked completely or nearly so in 10 μM TTX. This component is insensitive to known Ca^{2+} channel blockers but suppressed by 10 μM TTX, and so does not have the pharmacological profile of Ca^{2+} channels. We refer to this TTX-blockable Ca^{2+} current component as $I_{Ca(TTX)}$. All further observations on $I_{Ca(TTX)}$ were made in the presence of 10 μM La^{3+} to suppress L-type currents. $I_{Ca(TTX)}$ and I_{Na} were always extracted using TTX subtraction with 10 μM TTX.

$I_{Ca(TTX)}$ channels are permeable to Na^+ ions

Figure 5 presents current–voltage relations, obtained using TTX subtraction, from the same cell in 3 mM Ca_o^{2+}, 0 Na_o^+ (○), 3 mM Ca_o^{2+}, 1 mM Na_o^+ (□) and again in 3 mM Ca_o^{2+}, 0 Na_o^+ (△). $I_{Ca(TTX)}$ (○, △) reaches its maximum inward value about 8 mV more negative than does the current in the presence of both Na_o^+ and Ca_o^{2+}, suggesting that there may be more than one current component when both ions are present. That this is indeed the case is seen from an examination of the activation curves.

The peak current values of Fig. 5 were converted to peak conductances using the expression:

$$I_i = g_i(V - V_{rev}), \quad (1)$$

where I_i is current, g_i is conductance, V is potential and V_{rev} is the null potential for each ionic condition. Conductance as a function of potential, $g(V)$, for the initial 3 mM Ca_o^{2+}, 0 Na_o^+ values of Fig. 5 is shown as filled circles in Fig. 6*A*. The smooth curve is a best-fit Boltzmann function given by:

$$g(V) = g_{max}/(1 + \exp((V - V_{½})/k)), \quad (2)$$

with g_{max} (the maximum conductance) of 20·26 nS, $V_{½}$ (the potential at which $g(V) = \frac{1}{2}g_{max}$) of −47·6 mV and k (a slope factor) of −4·04 mV. The data of Fig. 6*A* are well described by a single Boltzmann function. Attempts to detect an additional component in these data could not define an additional Boltzmann function with reliable parameters. Hence, with only external Ca^{2+} present only a single component is detected in the TTX-blockable current. This same result was obtained in three additional cells, suggesting that classical cardiac Na^+ channels do not display any appreciable Ca^{2+} permeability or, under these conditions, generate any significant outward current.

Values of $g(V)$ for the 3 mM Ca_o^{2+}, 1 mM Na_o^+ data of Fig. 5 are shown as the filled circles of Fig. 7*A*. The smooth curve is again a best-fit single Boltzmann function with a g_{max} of 40·90 nS, a $V_{½}$ of −45·9 mV and a k of −4·16 mV. A single Boltzmann function does not provide a satisfactory description of these data. A substantially better description is provided by fitting with the sum of two Boltzmann functions. Figure 7*B* again presents the data of Fig. 7*A*. The smooth curve in Fig. 7*B* is a best-fit sum of two Boltzmann functions which includes a major component with a g_{max} of 26·26 nS, a $V_{½}$ of −49·3 mV and a k of −3·36 mV, and a

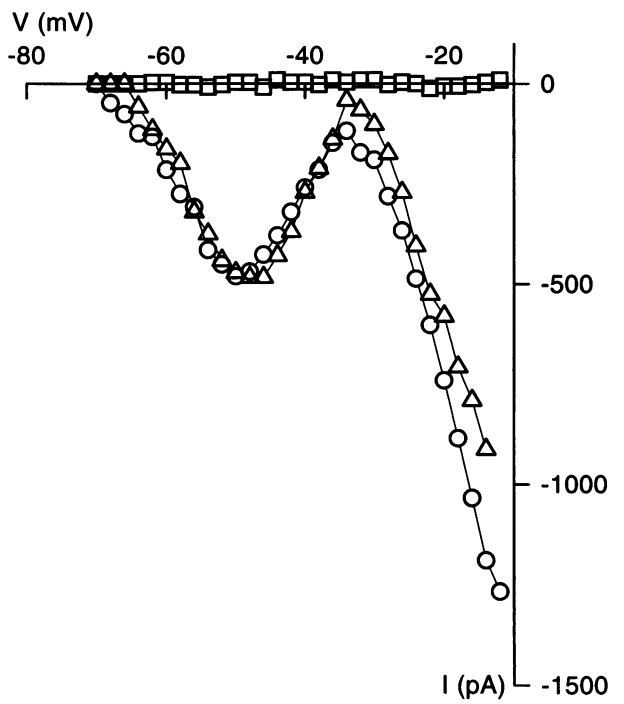

Figure 3. Peak current–voltage relations in the presence and absence of Ca_o^{2+}

Current–voltage relations, all from the same cell, in the presence (○), absence (□) and return (△) to 1 mM Ca_o^{2+}. Na_o^+ was 0 mM throughout. Holding potential was −100 mV. Both inward current components are carried by Ca^{2+} ions.

smaller component with a g_{max} of 13·86 nS, a $V_{½}$ of −40·8 mV and a k of −2·05 mV.

The larger component seen in the presence of both Na_o^+ and Ca_o^{2+} is nearly identical to the single component seen with Ca_o^{2+} alone. The larger component has a $V_{½}$ of −49·3 mV, while that for this same cell with only Ca^{2+} externally is −47·6 mV. Similarly, k for the larger component is −3·36 mV, while that with only Ca^{2+} is −4·04 mV. However, the smaller component seen in both Na_o^+ and Ca_o^{2+} is clearly distinct from that seen in Ca_o^{2+} alone, with a $V_{½}$ of −40·8 mV and a k of −2·05 mV.

This same result was obtained in two additional cells, and the data are summarized in Table 1. In each case the sum of two Boltzmann functions fitted in the presence of both Ca_o^{2+} and Na_o^+ yielded one (always larger under these experimental conditions) component that was nearly identical to that obtained in the presence of Ca_o^{2+} alone and a second that was clearly different. The mean $V_{½}$ and k for the larger component in both Na_o^+ and Ca_o^{2+} were −45·1 and −3·90 mV, respectively, compared with means of −44·5 and −4·49 mV for the corresponding values in Ca_o^{2+}, while mean values for the smaller component in Na_o^+ and Ca_o^{2+} were −35·6 and −2·31 mV, respectively. The smaller Boltzmann component contributes 20–35% of the total maximum conductance under these conditions and at, and negative to, about −45 mV constitutes a negligible fraction of the measured conductance, owing to the more negative range of activation of the larger component. Moreover, under these ionic conditions, the smaller component (which is seen only in the

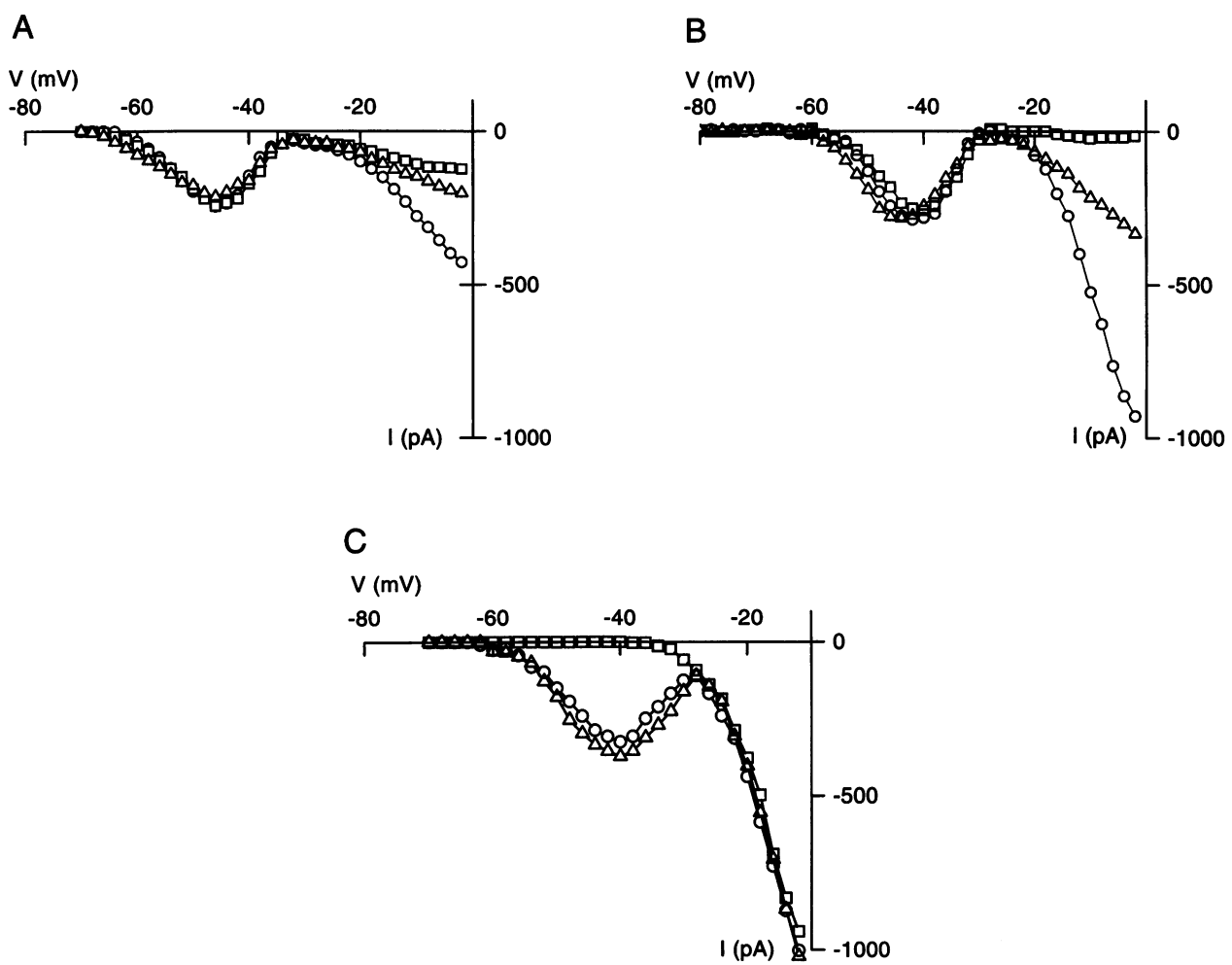

Figure 4. Effects of Ni^{2+}, La^{3+} and TTX on the more negative voltage range-activated inward current component

Each panel presents three peak current–voltage relations from one ventricular cell. Data are from a different cell in each panel. External bathing medium contained either 3 mM (*A* and *B*) or 1 mM (*C*) Ca_o^{2+} and 0 Na_o^+ throughout. Holding potential was −100 mV. In each part of the figure ○ represents values in external medium only, □ shows the effect of the indicated channel blocker and △ the values on return to external medium with no blocker. *A*, effect of 50 μM Ni^{2+}. *B*, effect of 10 μM La^{3+}. *C*, effect of 10 μM TTX. Neither of the Ca^{2+} channel blockers Ni^{2+} or La^{3+} affect the smaller, more negatively activated component. This component is, however, reversibly blocked by the Na^+ channel agent, TTX.

Table 1. Fit parameters for conductance–voltage, $g(V)$, relations in rat ventricular myocytes in the presence of 3 mM external Ca^{2+} and no Na^+ and in the presence of 3 mM external Ca^{2+} and 1 mM Na^+

	3 mM Ca_o^{2+}, 0 Na_o^+			3 mM Ca_o^{2+}, 1 mM Na_o^+					
				Component 1			Component 2		
Cell	$V_{½}$ (mV)	k (mV)	g_{max} (nS)	$V_{½}$ (mV)	k (mV)	g_{max} (nS)	$V_{½}$ (mV)	k (mV)	g_{max} (nS)
41796A	−47·6	−4·04	20·26	−49·3	−3·36	26·26	−40·8	−2·05	13·86
51596E	−42·6	−5·49	33·97	−43·1	−4·54	42·46	−32·8	−2·59	9·51
60596B	−43·4	−3·95	37·32	−42·8	−3·79	43·45	−33·1	−2·28	13·55
Mean	−44·5	−4·49	30·52	−45·1	−3·90	37·39	−35·6	−2·31	12·31

Fits were to single (3 mM Ca_o^{2+}, 0 Na_o^+) or to the sum of two Boltzmann functions (3 mM Ca_o^{2+}, 1 mM Na_o^+) as given by eqn (2) in the text.

presence of Na_o^+ and so presumably arises from classical Na^+ channels) is likely to display voltage-dependent block by external Ca^{2+} ions (Yamamoto, Yeh & Narahashi, 1984), which would produce an apparent steepening of its $g(V)$. k values for this component, then, may not be highly accurate. At, and positive to, about −35 mV, however, this component contributes a significant fraction of the measured conductance.

The close agreement of the $g(V)$ mid-point and slope suggests that the larger conductance component seen in Ca_o^{2+} plus Na_o^+ arises from the same channels that generate the $g(V)$ seen in Ca_o^{2+} alone. Comparing the fitted g_{max} values for this channel population under the two ionic conditions should, then, provide a fairly direct assessment of the permeability of $I_{Ca(TTX)}$ channels to Na^+ ions. For the cell of Figs 5–7, g_{max} in 3 mM Ca_o^{2+}, 0 Na_o^+ was 20·26 nS. Adding 1 mM Na_o^+ to the 3 mM Ca_o^{2+} increased g_{max} for this population of channels to 26·26 nS or by 29·6%, indicating that $I_{Ca(TTX)}$ channels are permeable to Na^+.

An effect on g_{max} this large is well beyond any that might be attributed to the variance in fitted parameters arising from the noise of the experimental data. Figure 6*B* again presents the $g(V)$ values of Fig. 6*A* in 3 mM Ca_o^{2+}, 0 Na_o^+. The smooth curve is a best-fit single Boltzmann function, now fitted with g_{max} constrained to be that of this same channel population in Na_o^+ plus Ca_o^{2+} (26·26 nS). The curve is clearly a poor description of the data. A g_{max} value of 26·26 nS is not consistent with the data recorded in Ca_o^{2+} alone. Correspondingly, it was not possible to produce a satisfactory fit to the $g(V)$ data in Na_o^+ plus Ca_o^{2+} by constraining one of the Boltzmann functions to have the g_{max}, $V_{½}$ and k values of the Ca_o^{2+} only data of Fig. 6*A*. Adjusting $V_{½}$ and k of the constrained Bolzmann function for the slight differences in these values in Na_o^+ plus Ca_o^{2+} compared with those in Ca_o^{2+}

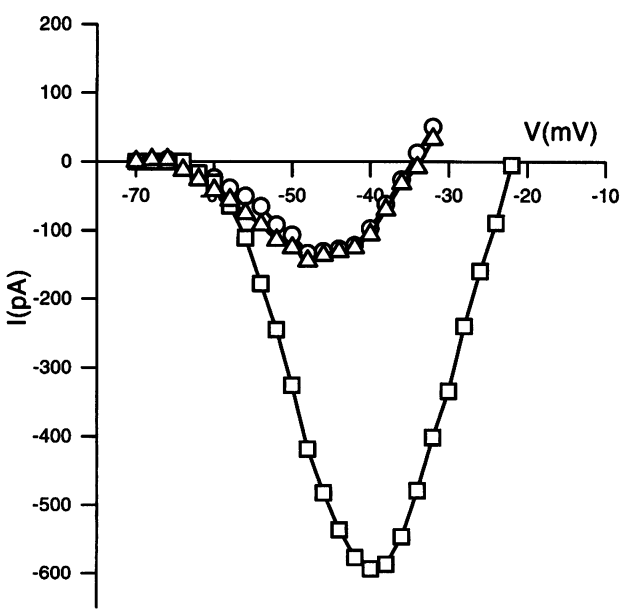

Figure 5. TTX-blockable currents in the presence of Ca_o^{2+} only and in Ca_o^{2+} plus Na_o^+

Three peak current–voltage relations from the same cell in the presence of 3 mM Ca_o^{2+}, 0 Na_o^+ (○), 3 mM Ca_o^{2+}, 1 mM Na_o^+ (□), and on return to 3 mM Ca_o^{2+}, 0 Na_o^+ (△) are shown. All values were obtained using TTX subtraction. Holding potential was −100 mV throughout.

only did not produce a satisfactory fit either (not illustrated). Hence, the data in Ca_o^{2+} only are incompatible with a g_{max} of 26·26 nS, and those in Ca_o^{2+} plus Na_o^+, for these same channels, are incompatible with a g_{max} of 20·26 nS. Adding 1 mM Na_o^+ increases the conductance of $I_{Ca(TTX)}$ channels over that seen in 3 mM Ca_o^{2+} only. Nor is it possible to attribute the increased g_{max} of this channel population to some change in channel properties during the course of the experiment. On return from 3 mM Ca_o^{2+}, 1 mM Na_o^+ back to 3 mM Ca_o^{2+}, 0 Na_o^+ the current–voltage relation was nearly identical to that seen before exposure to Na_o^+ (Fig. 5, ○, △). $I_{Ca(TTX)}$ channels are permeable to Na^+. Similar results were obtained for the other two cells analysed (Table 1). The mean increase in g_{max} in the three cells on adding 1 mM Na_o^+ to 3 mM Ca_o^{2+} was 23·7 %. $I_{Ca(TTX)}$ channels are insensitive to the Ca^{2+} channel blockers Ni^{2+} and La^{3+}, blocked by the Na^+ channel agent, TTX, and permeable to Na^+ ions. They are, then, Na^+ channels.

Another conclusion following from the close agreement of the larger Boltzmann component seen in Ca_o^{2+} and Na_o^+ with that seen in Ca_o^{2+} alone is that any residual uncompensated series resistance (or any other voltage clamp errors associated with the current magnitude) could not have had any appreciable effect on these data. For the experiment of Fig. 5, the maximum inward current in Na_o^+ plus Ca_o^{2+} is more than fourfold greater than that in Ca_o^{2+} alone. Nevertheless $V_{½}$ and k for $I_{Ca(TTX)}$ channels in the two conditions are nearly identical.

$I_{Ca(TTX)}$ Na^+ channels are functionally distinct from classical rat ventricular Na^+ channels

$I_{Ca(TTX)}$ channels differ from classical cardiac Na^+ channels in their gating as well as their permeability properties. As shown in Table 1, $I_{Ca(TTX)}$ activates over a more negative range of potentials than the classical cardiac I_{Na}. Compared under the same conditions, the mid-point of the activation curve is nearly 10 mV more negative for $I_{Ca(TTX)}$ ($V_{½}$ of

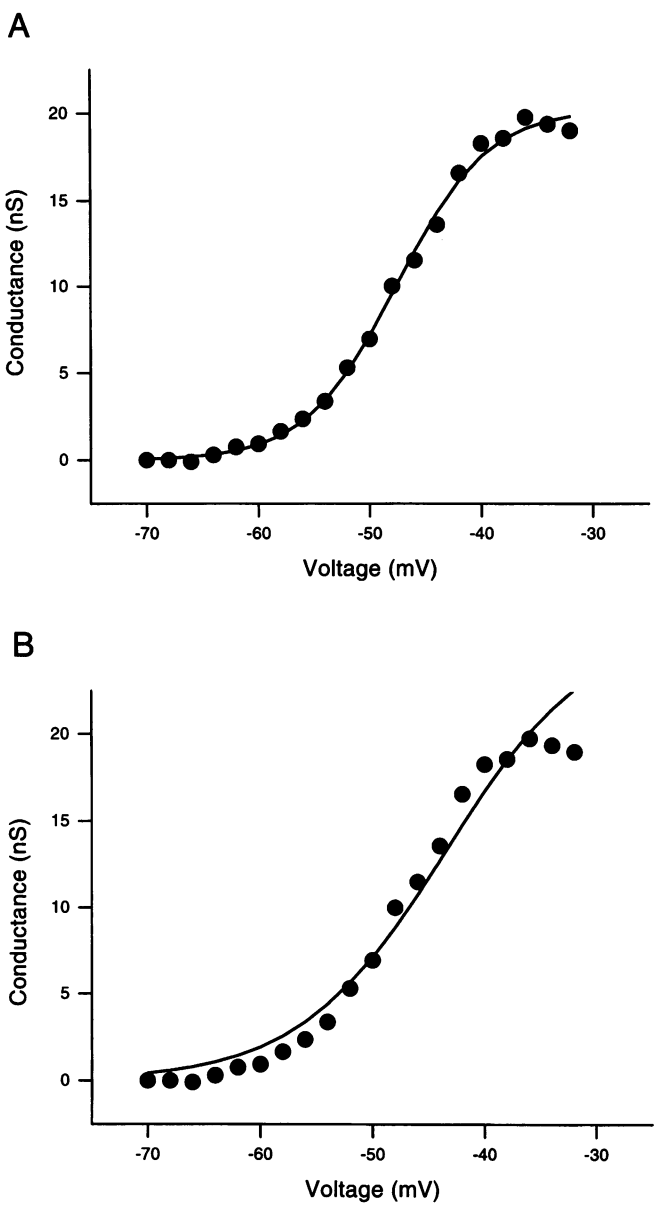

Figure 6. Conductance–voltage relation for the TTX-blockable current in the presence of Ca_o^{2+} only

A, peak conductance–voltage relation for the cell of Fig. 5 (○) in the presence of 3 mM Ca_o^{2+}, 0 Na_o^+. Smooth curve is a best-fit Boltzmann function (see text) with $V_{½}$ of −47·6 mV, k of −4·04 mV and g_{max} of 20·26 nS. *B*, ● are the same conductance values shown in *A*. Smooth curve is a single Boltzmann function fitted with g_{max} constrained to be that of the corresponding component of Fig. 7*B* (26·26 nS). The smooth curve is a poor description of these data.

−45·1 mV compared with −35·6 mV for the classical I_{Na}). Activation characteristics are therefore distinct for these two Na^+ current components.

$I_{Ca(TTX)}$ also inactivates over a more negative range of potentials than the classical I_{Na}. In four cells the steady-state inactivation curve was determined in 3 mM Ca_o^{2+}, 0 Na_o^+ and again in 3 mM Ca_o^{2+} plus 2 mM Na_o^+. One example is shown in Fig. 8. Potential was stepped from a holding potential of −100 mV to various conditioning pulse levels ranging from −130 to −35 mV. After 150 ms at the conditioning level, potential was stepped to −30 mV and the peak current during this test step was determined. Figure 8 presents these peak currents, normalized to the maximum value seen, as a function of conditioning potential. The smooth curves are best fits to the expression:

$$I/I_{max}(V) = (1 + \exp((V - V')/k'))^{-1}, \quad (3)$$

where V' is the potential at which $I/I_{max} = \frac{1}{2}$. $I/I_{max}(V)$ is clearly different in the two ionic conditions. In the presence of both Ca_o^{2+} and Na_o^+ (▽), V' and k' are −77·7 and 7·61 mV, respectively, while the corresponding values in Ca_o^{2+} only (△) are −84·6 and 9·06 mV. Similar results were obtained in the other three cells studied, and values are presented in Table 2. V' ranged from 4·6 to 9·9 mV more negative in Ca_o^{2+} compared with Ca_o^{2+} plus Na_o^+, with a mean in Ca_o^{2+} only of −83·1 mV and in Ca_o^{2+} plus Na_o^+ of −75·4 mV. k' ranged from 0·51 to 2·01 mV larger in Ca_o^{2+} compared with that in Ca_o^{2+} and Na_o^+, with a mean of 8·34 mV in Ca_o^{2+} only and of 6·85 mV in the presence of both ions. Note that these values do not reflect the full difference in steady-state inactivation characteristics in $I_{Ca(TTX)}$ compared with classical cardiac Na^+ channels as the data in Ca_o^{2+} plus Na_o^+ will include contributions from both current components.

Table 2. Fit parameters for steady-state inactivation, $I/I_{max}(V)$, curves in rat ventricular myocytes in the presence of 3 mM external Ca^{2+} and no Na^+ and in the presence of 3 mM external Ca^{2+} and 2 mM Na^+

Cell	3 mM Ca_o^{2+}, 0 Na_o^+		3 mM Ca_o^{2+}, 2 mM Na_o^+	
	V' (mV)	k' (mV)	V' (mV)	k' (mV)
62096B	−79·2	8·86	−74·6	6·85
62096C	−83·8	8·43	−73·8	6·44
70296A	−84·9	7·01	−75·4	6·50
71996A	−84·6	9·06	−77·7	7·61
Mean	−83·1	8·34	−75·4	6·85

Fits were to eqn (3) in the text.

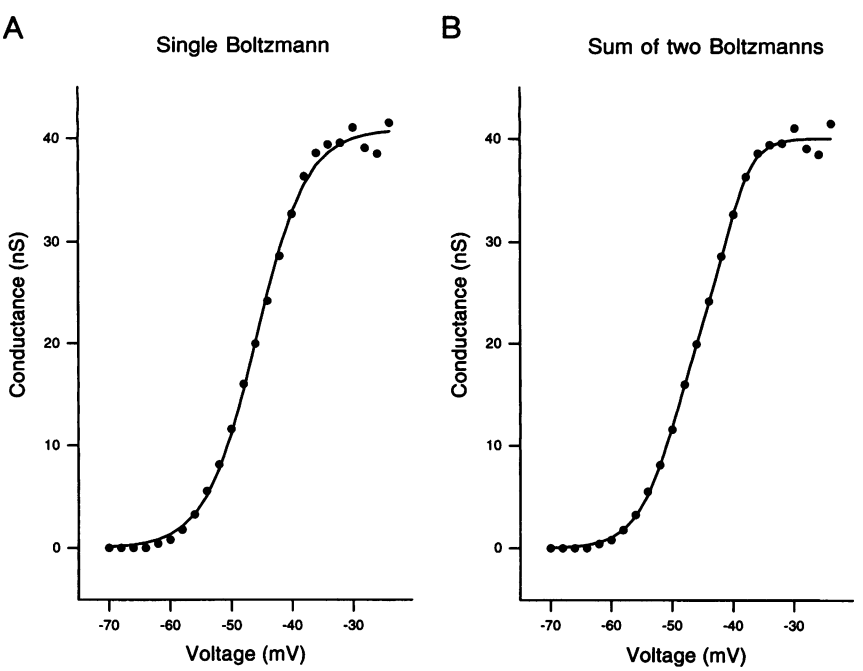

Figure 7. Conductance–voltage relation for the TTX-blockable current in the presence of Ca_o^{2+} plus Na_o^+

Both panels present the peak conductance voltage values for the cell of Fig. 5 (□) in the presence of 3 mM Ca_o^{2+} plus 1 mM Na_o^+. *A*, smooth curve is a best-fit single Boltzmann function with $V_{½}$ of −45·9 mV, k of −4·16 mV and g_{max} of 40·90 nS. *B*, smooth curve is a best-fit sum of two Boltzmann functions. One component was fitted with $V_{½}$ of −49·3 mV, k of −3·36 mV and g_{max} of 26·26 nS. The other was fitted with $V_{½}$ of −40·8 mV, k of −2·05 mV and g_{max} of 13·86 nS. A sum of two Boltzmann functions provides a better description of these data than does a single Boltzmann function.

Inactivation kinetics are slower in $I_{Ca(TTX)}$ than in the classical cardiac I_{Na}. Figure 9 presents current records from the same cell in the presence of 1 mM Ca_o^{2+} and 0 Na_o^+ (left column) and in 0 Ca_o^{2+} and 1 mM Na_o^+ (middle column). Potentials were stepped from a holding value of −100 mV to the values indicated at the left of the traces. At each potential, current decays more slowly in Ca_o^{2+} than in Na_o^+. This is shown more clearly in the right-hand column. In this column the records in Na_o^+ are again shown now with those recorded in Ca_o^{2+} superimposed. The Ca_o^{2+} records have been scaled up so that their peaks match those in Na_o^+ at each potential. Inactivation is slower in Ca_o^{2+} than in Na_o^+.

The time constant of inactivation, τ_h, was determined from single-exponential fits to the decaying phase of the currents. Mean τ_h values, pooled from four cells in Ca_o^{2+} (○) and four in Na_o^+ (□), are shown in Fig. 10. τ_h in Ca_o^{2+} is slower than that in Na_o^+ at every potential studied.

Values of τ_h were also determined in six cells in the presence of both Ca_o^{2+} (0·5 mM) and Na_o^+ (1 mM). Under these conditions, two relaxations in the decay of the current could be detected at more negative potentials. Figure 11 shows one example for a step to −55 mV. Fitting a single exponential to the current decay from 7·8 to 25·0 ms into the step in potential (Fig. 11, upper trace, smooth curve) yielded a τ_h of 3·83 ms. This fitted exponential did not describe the current at earlier times. Fitting a single exponential over the interval 2·4–4·2 ms (middle trace, smooth curve) yielded a faster τ_h of 2·70 ms, but did not correctly describe the current decay at longer times. The whole decay time course could be well described by a two-exponential fit (bottom trace, smooth curve) with a $\tau_{h,fast}$ of 2·68 ms and $\tau_{h,slow}$ of 6·92 ms. Mean values for these double-exponential fits are also shown in Fig. 10 (▽, $\tau_{h,fast}$; △, $\tau_{h,slow}$). $\tau_{h,slow}(V)$ agrees closely with the single-exponential $\tau_h(V)$ values seen in Ca_o^{2+} only, and $\tau_{h,fast}(V)$ is also very similar to the single-exponential fit values obtained in Na_o^+ only. Hence, the slow τ_h seen in Ca_o^{2+} only cannot be attributed to any shift in values along the voltage axis that might be produced on changing from 0 to 1 mM Ca_o^{2+}. The different inactivation kinetics do not arise from the different ionic conditions. Another result following from the close agreement between $\tau_{h,slow}$ and the single-exponential τ_h values in Ca_o^{2+} only is that, again, these data cannot be affected to any appreciable extent by any residual uncompensated series resistance effects. Mean peak currents in 0·5 mM Ca_o^{2+} plus 1 mM Na_o^+ were four- to fivefold larger than those in Ca_o^{2+} only, but the $I_{Ca(TTX)}$ inactivation time course was the same in the two bathing media.

Brown, Lee & Powell (1981) also found two inactivation relaxations in the I_{Na} of rat ventricular myocytes, and their $\tau_{h,fast}(V)$ and $\tau_{h,slow}(V)$ values are in reasonable agreement with those reported here. Brown *et al.* (1981) recorded in the presence of Na_o^+ but no Ca_o^{2+}. Their $\tau_{h,slow}$ component, then, is very likely generated by Na^+ ions flowing through $I_{Ca(TTX)}$ channels, in agreement with the conclusion of Figs 6 and 7 and Table 1 that $I_{Ca(TTX)}$ channels are permeable to Na^+ ions. We detected only a single inactivation relaxation in Na_o^+ only as our Na_o^+ concentration was fiftyfold or more lower than those used by Brown *et al.* (1981), and the slower inactivation component, which is very small relative to the faster (Brown *et al.* 1981), was not resolvable with the relatively small current amplitudes of our experiments.

The close agreement between $\tau_{h,fast}$ and τ_h in Na_o^+ only at more negative potentials might seem surprising considering the data of Table 1. From the mean $V_{½}$ and k values of the $g(V)$ fits in Ca_o^{2+} plus Na_o^+ at, and negative to, −50 mV $I_{Ca(TTX)}$ channels should contribute appreciably to the total g_{Na} even if classical I_{Na} channels are substantially more frequent than $I_{Ca(TTX)}$ channels. The single-exponential τ_h in Na_o^+ only, then, might be expected to be weighted significantly by the more slowly inactivating $I_{Ca(TTX)}$. However, the experiments of Table 1 were done in 3 mM Ca_o^{2+}, while all τ_h determinations were in 0–1 mM Ca_o^{2+}. For the τ_h experiments, then, $V_{½}$ values of activation for both $I_{Ca(TTX)}$ and classical Na^+ channels, and hence the potential range over which $I_{Ca(TTX)}$ channels dominate the total activated g_{Na}, should be shifted to more negative values. Hence, over the potential range examined for the τ_h determinations, the contribution of $\tau_{h,slow}$ to the single-exponential τ_h is actually expected to be modest at best and to

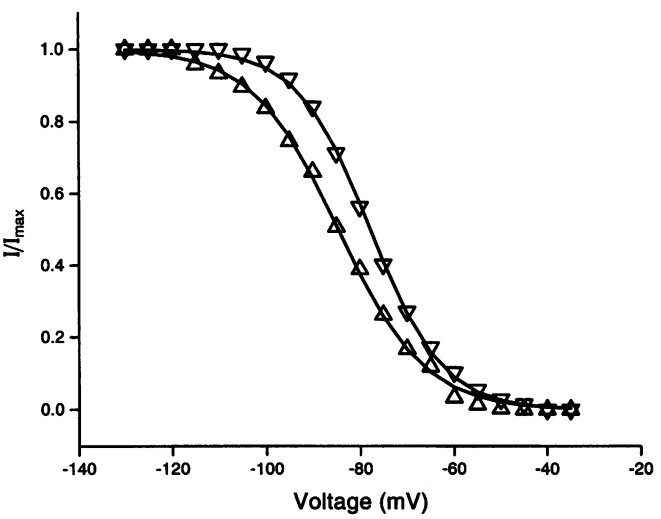

Figure 8. Steady-state inactivation curves in Ca_o^{2+} only and in Ca_o^{2+} plus Na_o^+

Peak current values during a −30 mV test step in potential are shown. Each test step was preceded by a 150 ms conditioning step to one of the indicated potentials. Peak currents are normalized to the maximum value seen for each condition. Two curves, both from the same cell, are shown. Values were obtained in 0 Na_o^+, 3 mM Ca_o^{2+} (△) and in 2 mM Na_o^+, 3 mM Ca_o^{2+} (▽). Smooth curves are best fits to eqn (3) in the text with V' of −77·7 mV and k' of 7·61 mV (▽) and V' of −84·6 mV and k' of 9·06 mV (△). Values were obtained using TTX subtraction.

decrease to a negligible level at more positive potentials. An upper limit to the contribution of $\tau_{h,slow}$ to the single-exponential τ_h can be estimated by comparing, for the six cells exposed to 0·5 mM Ca_o^{2+} plus 1 mM Na_o^+ of Fig. 10, single-exponential $\tau_h(V)$ fits to $\tau_{h,fast}(V)$ of the double-exponential fits. Mean ratio of τ_h (single-exponential fit) to $\tau_{h,fast}$ for those six cells was: 1·73 at −55 mV, 1·43 at −50 mV, 1·30 at −45 mV and 1·10 at −40 mV. Thus, under these experimental conditions the slowly inactivating $I_{Ca(TTX)}$ does weight the single-exponential τ_h moderately to negligibly. Moreover, in Na_o^+ only, the weight of the slowly inactivating component should be even less as the current carried by $I_{Ca(TTX)}$ channels will be reduced substantially by removing Ca_o^{2+}, while that through the classical I_{Na} channels is expected to increase, especially at more negative potentials (Yamamoto *et al.* 1984). Brown *et al.* (1981) also found that the slower inactivation relaxation seen in Na_o^+ only was considerably smaller in amplitude than the faster, and contributed negligibly to the single-exponential τ_h positive to about −50 mV. Hence, the $\tau_h(V)$ values in Na_o^+ only of Fig. 10 are expected to be only slightly weighted by the slower inactivating $I_{Ca(TTX)}$ channels under those conditions and so agree closely with $\tau_{h,fast}(V)$.

Compared with classical cardiac Na^+ channels $I_{Ca(TTX)}$ channels activate and inactivate over more negative potential ranges, have a less steep voltage dependency for both activation and inactivation, slower inactivation kinetics, and very different permeability properties. Hence, $I_{Ca(TTX)}$ is a Na^+ current component clearly distinct in its characteristics from the classical cardiac I_{Na}, and probably, then, also in its functional role.

The ratios of the zero time intercepts of the two exponential components in the double-exponential fits of Figs 10 and 11 provide a rough estimate of the relative contribution of the two Na^+ current components. This method overestimates the contribution of the faster component, and this error increases as the values of the two time constants become more divergent. Nevertheless, some information can be gained. The mean value of the ratio of the zero time intercepts at −55 mV (fast to slow) was 5·36 in the presence of low concentrations of both Na_o^+ and Ca_o^{2+}. There was a tenfold range of values at this potential, from 1·36 to 13·9. It is not possible, however, to attribute this wide range of variation to differences in the relative values of the two time constants. The cell with the fast to slow intercept ratio of 1·36 had a faster $\tau_{h,fast}$ (2·72 *vs.* 2·95 ms) and a slower $\tau_{h,slow}$ (14·25 *vs.* 11·00 ms) than the cell with the ratio of 13·9. There seems, then, to be a wide variability from cell to cell in the relative densities of $I_{Ca(TTX)}$ and classical I_{Na} channels. This wide variability in relative densities is more consistent with separate, non-interconvertable channel types than with the reversible conversion of some fraction of a single channel type into a different gating state (i.e. 'modes'; Patlak & Ortiz, 1985). It is not clear, however, how much of this wide variation in the relative abundance of these two channel types would be found *in situ*, and how much arises during the cell dissociation and experimental procedures.

Other properties of $I_{Ca(TTX)}$ channels

The block of inward currents produced by 0·1, 0·5, 1 and 2 μM TTX was examined in the presence of 2 mM Na_o^+ plus 0·5 mM Ca_o^{2+}. Thirteen determinations on seven cells were

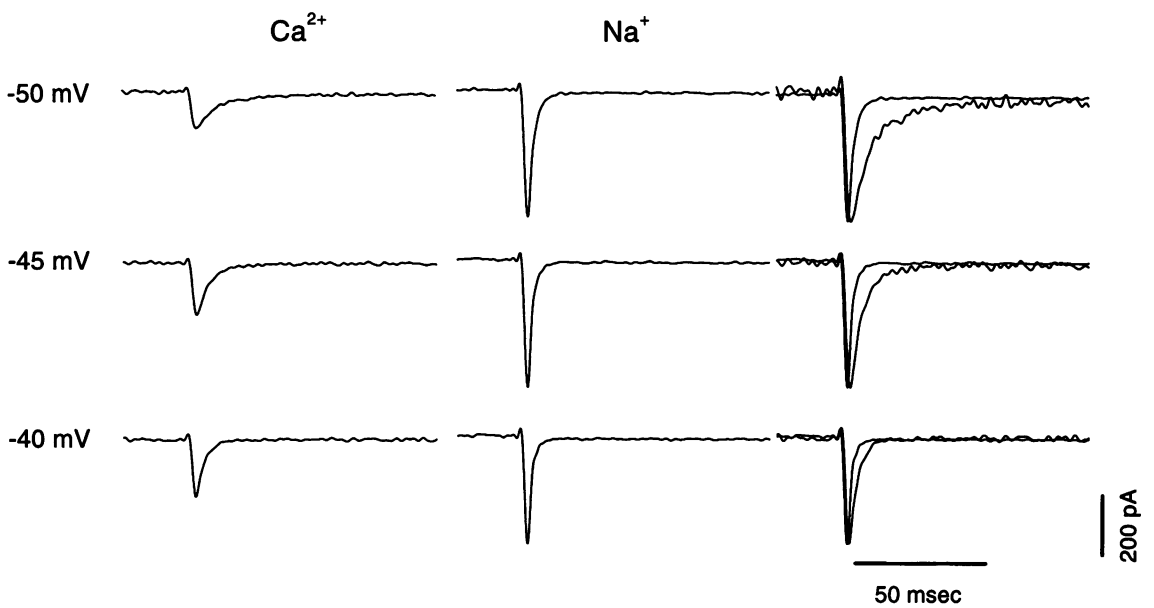

Figure 9. Current time course in Ca_o^{2+} and in Na_o^+

The left column presents three current traces, all from the same cell, recorded in 1 mM Ca_o^{2+} and 0 Na_o^+. Currents from this same cell at the same three potentials, now in 0 Ca_o^{2+} and 1 mM Na_o^+ are shown in the centre column. The right column again presents the records in 0 Ca_o^{2+}, 1 mM Na_o^+ now with those in 1 mM Ca_o^{2+}, 0 Na_o^+ recorded at that same potential superimposed. The records in Ca_o^{2+} have been scaled up so that their peaks match those recorded in Na_o^+. Inactivation kinetics are slower in Ca_o^{2+}. Records are TTX subtracted.

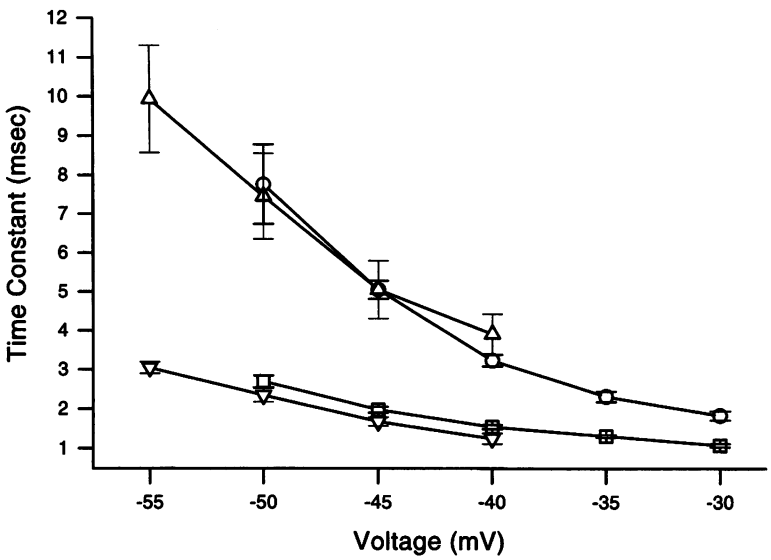

Figure 10. Inactivation time constants as a function of potential in Ca_o^{2+} only, Na_o^+ only and in Ca_o^{2+} plus Na_o^+

Time constants were obtained with either single (○, □) or double (△, ▽) exponential fits to the decay of the current. Currents were recorded in 1 mM Ca_o^{2+}, 0 Na_o^+ (○), 0 Ca_o^{2+}, 1 mM Na_o^+ (□) and 0·5 mM Ca_o^{2+}, 1 mM Na_o^+ (slow component, △; fast component, ▽). Analysis was on TTX-subtracted records. Values pooled from four cells in Ca_o^{2+} only, four in Na_o^+ only and six in Ca_o^{2+} plus Na_o^+. Bars indicate S.E.M.

made under these conditions. An effective dissociation constant, K_D, was determined from the mean value of the unblocked fraction of the TTX-blockable inward current, $I_{TTX}/I_{control}$, at each TTX concentration, assuming a single class of binding sites. K_D was computed from:

$$I_{TTX}/I_{control} = (1 + ([TTX]/K_D))^{-1}, \quad (4)$$

where [TTX] is the concentration of blocker used. There was no obvious trend in mean K_D values with concentration. K_D was 0·63 μM in 0·1 μM TTX (mean of three cells), 0·53 μM in 0·5 μM TTX (mean of four cells), 0·60 μM in 1 μM TTX (mean of four cells), and 0·84 μM in 2 μM TTX (mean of two cells), providing, then, no indication of more than one class of sites. These experiments are probably not sufficient to identify a population of high affinity sites constituting only a very small fraction of the total. Overall mean K_D under these conditions was 0·62 μM.

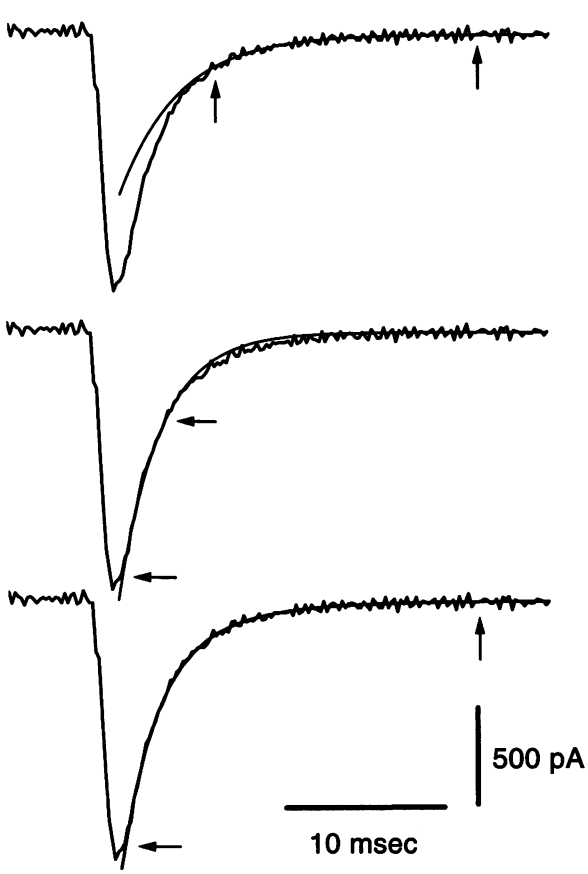

Figure 11. The TTX-subtracted current displays two inactivation relaxations in the presence of both Na_o^+ and Ca_o^{2+}

The same TTX-subtracted current trace recorded at −55 mV is presented three times. The smooth curve in the upper trace is a single-exponential fitted between 7·8 and 25·0 ms (indicated by arrows). That in the middle record is a single exponential fitted between 2·4 and 4·2 ms (arrows). The smooth curve in the lower record is a double exponential again fitted over the interval indicated by the arrows. Fitted time constant values were 3·83 ms (upper trace), 2·70 ms (middle trace) and 2·68 and 6·92 ms (lower trace).

TTX sensitivity was also examined in the presence of 3 mM Ca_o^{2+} and 0 Na_o^+, in 0·1, 1 and 2 μM TTX. Effective K_D values, again assuming only a single class of binding sites, were 0·66 μM in 0·1 μM TTX (mean of three cells), 1·16 μM in 1 μM TTX (mean of four cells), and 1·11 μM in 2 μM TTX (mean of three cells). Overall mean K_D was 1·00 μM, a value not different from that seen in Ca_o^{2+} plus Na_o^+.

In five cells $I_{Ca(TTX)}$ was recorded during long-lasting steps in potential (500–1500 ms), over the range −30 to −40 mV, to see if a persistent component could be identified. Five millimolar Ca_o^{2+} (with no Na_o^+) was used throughout. Peak inward $I_{Ca(TTX)}$ ranged from −450 to more than −800 pA, but in no case could a persistent current be detected. Figure 12*A* presents a current record from one such experiment. The first 125 ms of a 500 ms step to −30 mV are shown. Peak inward current was −570 pA, and this current seemed to inactivate completely. The continuous line indicates zero current. As little as −10 pA of inward current would have been readily detectable in this experiment. Figure 12*B* presents this same trace from 50 to 260 ms into the step, at an expanded current scale, now digitally filtered at 1 kHz. The continuous line again indicates zero current and the dashed line indicates −10 pA, which is measurably different from zero.

DISCUSSION

$I_{Ca(TTX)}$ in rat ventricular myocytes is not generated by either L- or T-type Ca^{2+} channels. The channels producing this current are also distinct from the classical rat ventricular cell Na^+ channels. They have different kinetics, different voltage ranges for activation and inactivation, and different permeability properties from the classical cardiac Na^+ channels, indicating that rat ventricular cells express more than one Na^+ current component. More than one kind of Na^+ current has now been reported for a wide variety of cell types (see below). For cardiac cells in particular, more than one functionally distinct type of Na^+ channel is a relatively common and possibly even a general feature. The frequency with which more than one type of Na^+ channel is encountered in cardiac and other excitable cells suggests that multiple Na^+ channel types may be a feature of some functional importance, not just for cardiac excitation and conduction but possibly for excitable cells quite broadly.

From tracer flux studies, it has long been known that Ca^{2+} ions enter squid giant axons during the generation of the action potential (Hodgkin & Keynes, 1957). This Ca^{2+} entry is largely or entirely through TTX-blockable channels (Watanabe, Tasaki, Singer & Lerman, 1967), and using the Ca^{2+} indicator, aequorin, Baker, Hodgkin & Ridgeway

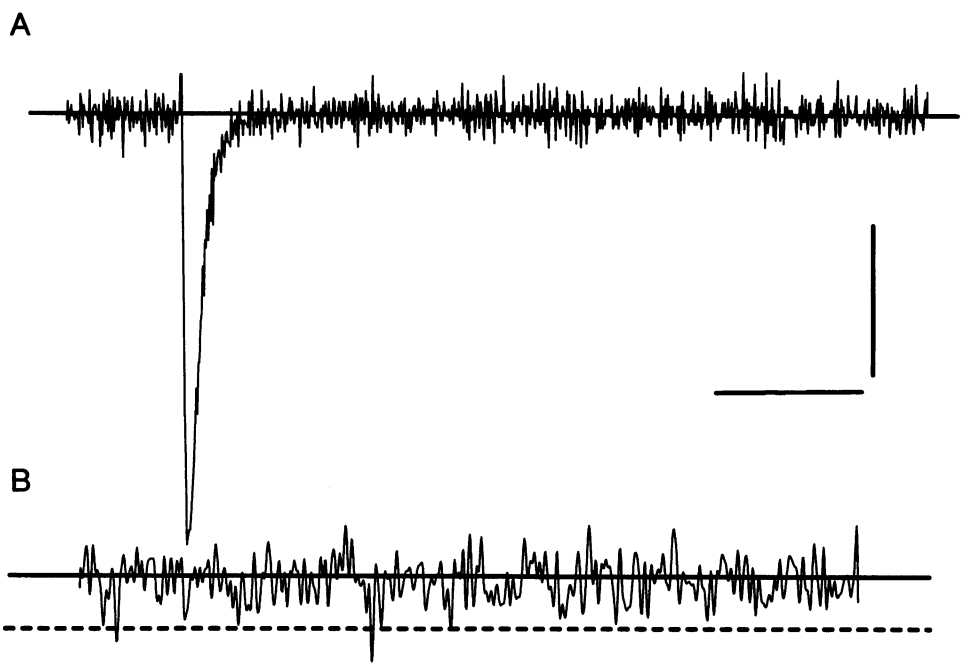

Figure 12. $I_{Ca(TTX)}$ does not display a persistent component

A current record during a step to −30 mV from a holding potential of −100 mV in the presence of 5 mM Ca_o^{2+} and no Na_o^+ is shown. *A*, recording of the first 125 ms of a 500 ms step; *B*, this same record from 50 to 260 ms into the step, now at higher gain. The record in *B* has been digitally filtered at 1 kHz. For both *A* and *B* the continuous line indicates the zero current level. The dashed line in *B* indicates −10 pA. $I_{Ca(TTX)}$ inactivates to a current level not detectably different from zero. Scales: 200 pA and 25 ms for *A*, and 30 pA and 40 ms for *B*.

(1971) found that an early phase of voltage-dependent Ca^{2+} entry in squid giant axons was blocked by TTX. Meves & Vogel (1973), also working on squid giant axons, described a small Ca^{2+} current that was blocked by TTX. $I_{Ca(TTX)}$ have also been reported in rat hippocampal CA1 cells (Akaike & Takahashi, 1992), human atrial cells (Lemaire *et al.* 1995), guinea-pig ventricular myocytes (Leblanc *et al.* 1996) and here in rat ventricular myocytes.

$I_{Ca(TTX)}$ flows through a subpopulation of Na^+ channels

$I_{Ca(TTX)}$ is insensitive to the Ca^{2+} channel blockers nifedipine (Leblanc *et al.* 1996), La^{3+} (Akaike & Takahashi, 1992; Lemaire *et al.* 1995; this study) and Ni^{2+} (Lemaire *et al.* 1995; this study), but modified by Na^+ channel agents such as scorpion toxin (Akaike & Takahashi, 1992) and veratridine (Lemaire *et al.* 1995; Leblanc *et al.* 1996). $I_{Ca(TTX)}$ channels have been shown to be permeable to Na^+ (Meves & Vogel, 1973; Akaike & Takahashi, 1992; this study). $I_{Ca(TTX)}$ seems, then, to flow through Na^+ channels.

$I_{Ca(TTX)}$ channels appear to be a distinct subpopulation from the main population of Na^+ channels in each cell type. They typically (i) display slower inactivation kinetics (Meves & Vogel, 1973; Akaike & Takahashi, 1992; Lemaire *et al.* 1995; this study), (ii) activate over more negative potential ranges (Meves & Vogel, 1973; Akaike & Takahashi, 1992; this study), and (iii) generate currents that are small relative to those produced by the main Na^+ channel population (Meves & Vogel, 1973; Lemaire *et al.* 1995; this study). Moreover, Lemaire *et al.* (1995), working on human atrial cells, found that neither the magnitude nor even the presence or absence of the $I_{Ca(TTX)}$ correlated with that of the classical I_{Na} from cell to cell, consistent with the view that $I_{Ca(TTX)}$ is generated by a population of channels separate from the main Na^+ channel type. Similarly, we also find a wide variation in the relative abundance of $I_{Ca(TTX)}$ and classical cardiac Na^+ channels in rat ventricular cells, suggesting that these two functional Na^+ current components do not reflect different gating modes of a single channel type (Patlak & Ortiz, 1985). Meves & Vogel (1973) had in fact proposed that there are two populations of Na^+ channels in squid axons with the small population showing a relatively large and the main population showing little or no Ca^{2+} permeability.

Distinct subpopulations of Na^+ channels are found in many cell types

There are a number of additional clear demonstrations of more than one type of Na^+ or at least TTX-blockable current in a single cell type. Compelling evidence for another Na^+ channel type has been reported in *Myxicola* giant axons (Goldman & Hahin, 1978), denervated (Pappone, 1980), cultured (Gonoi, Sherman & Catteral, 1985), and developing (Weiss & Horn, 1986) rat skeletal muscle, rat ventricular cells (Cachelin *et al.* 1983; Kunze *et al.* 1985; Saint *et al.* 1992; Ju, Saint & Gage, 1994; this study), squid giant axons (Gilly & Armstrong, 1984), chick ventricular myocytes (Ten Eick *et al.* 1984), frog myelinated axons (Benoit, Corbier & Dubois, 1985), canine cardiac Purkinje fibres (Scanley & Fozzard, 1987), rat cultured type-2 astrocytes (Barres, Chun & Corey, 1989), rat cortical neurons (Kirsch & Brown, 1989), human neuroblastoma LA-N-5 cells (Weiss & Sidell, 1991), human atrial cells (Sakakibara *et al.* 1992), and rabbit Purkinje and ventricular cells (Zilberter *et al.* 1994).

Compared with the main body of Na^+ channels, the additional (i.e. less frequent) type of Na^+ channel displays some diverse properties. For example, it requires more positive conditioning potentials to produce inactivation than the main population in squid axons (Meves & Vogel, 1973) and frog myelinated axons (Benoit *et al.* 1985), but less positive in denervated muscle (Pappone, 1980), rat type-2 astrocytes (Barres *et al.* 1989), human LA-N-5 cells (Weiss & Sidell, 1991), and rat ventricular myocytes (this study). However, two characteristics are encountered with notable frequency. The additional type of Na^+ channel typically (i) displays slower inactivation kinetics than the main Na^+ channel population (Goldman & Hahin, 1978; Pappone, 1980; Benoit *et al.* 1985; Barres *et al.* 1989; Kirsch & Brown, 1989; this study), and (ii) activates over more negative potential ranges (Goldman & Hahin, 1978; Pappone, 1980; Gilly & Armstrong 1984; Benoit *et al.* 1985; Weiss & Horn, 1986; Barres *et al.* 1989; Weiss & Sidell, 1991; Saint *et al.* 1992; Ju *et al.* 1994; Zilberter *et al.* 1994; this study).

Hence, an additional type of Na^+ channel has been reported in *Myxicola* and squid giant axons, frog myelinated axons, rat hippocampal CA1 cells, rat cortical neurons, rat cultured type-2 astrocytes, human cultured neuroblastoma cells, developing and denervated rat skeletal muscle, ventricular myocytes in chick, guinea-pig and rat, canine cardiac Purkinje fibres, human atrial cells, and rabbit Purkinje and ventricular cells. This widespread occurrence suggests that the expression of more than one functional type of Na^+ channel may be of significance for the physiology of at least some of these diverse cells. That (in each case where data was available for comparison) the additional type of I_{Na} displayed slower inactivation kinetics and activated over a more negative potential range than the main I_{Na} component suggests that it may fill a similar functional role in diverse cell types.

The second type of Na^+ channel may not be identical across all cell types, however. Values for the sensitivity of this second Na^+ channel to TTX ranged from a concentration needed to block half the current, IC_{50}, of 3·5 nM in rat hippocampal CA1 cells (Akaike & Takahashi, 1992) to a K_D greater than 6 μM in human neuroblastoma cells (Weiss & Sidell, 1991). Moreover, the *second* (i.e. less frequent) type of Na^+ channel in rat skeletal muscle may be encoded by the same gene, *SkM2*, that encodes the *main* type in rat ventricular cells (Rogart, Cribbs, Muglia, Kephart & Kaiser, 1989; Kallen, Sheng, Yang, Chen, Rogart & Barchi, 1990). A closely matching isoform has also been isolated from human adult cardiac tissue (Gellens *et al.* 1992). While it is

not completely clear that it is the main (as opposed to some other) cardiac Na^+ channel that is identical to the second skeletal muscle channel, the more than thousandfold range of reported TTX sensitivities suggests that even if the second Na^+ channel type has a similar functional role in diverse cell types, it may not always be structurally identical. A question of interest for cardiac electrophysiology is the nature of the additional Na^+ channel or channels in cardiac cells.

A second, smaller I_{Na} component has also been reported in dorsal root ganglion neurons (Ogata & Tatebayashi, 1992; Roy & Narahashi, 1992). This second Na^+ component in rat dorsal root ganglion neurons displays massively slowed both inactivation and activation kinetics compared with the main channel type, and activates over a more positive range of potentials (Ogata & Tatebayashi, 1992; Roy & Narahashi, 1992). It has a remarkably high K_D for TTX, 100 μM (Roy & Narahashi, 1992) or higher (Ogata & Tatebayashi, 1992) and so is clearly divergent in properties from the other I_{Na} components discussed here. A similar divergent additional I_{Na} component with little or no demonstrated TTX sensitivity has been reported in other vertebrate peripheral neurons (e.g. Bossu & Feltz, 1984).

More than one type of Na^+ channel in mammalian cardiac cells

Evidence for more than one type of mammalian cardiac Na^+ current has been accumulating for some time. Coraboeuf, Deroubaix & Coulombe (1979) found that the action potential duration in canine cardiac Purkinje fibres was shortened by TTX concentrations (30–60 nM) that had no effect on the maximum rate of rise of the action potential, $\dot{V}_{max}$, consistent with a second small population of slower inactivating or persistent Na^+ channels with a higher TTX sensitivity than the main population. While action potential duration and $\dot{V}_{max}$ may not be equally sensitive assays of I_{Na} magnitude, subsequent studies supported the idea of more than one Na^+ channel population in cardiac cells. In rat ventricular myocytes Saint *et al.* (1992) found that a small I_{Na} component that did not fast inactivate was more TTX sensitive than the large, rapidly inactivating component. It also activated over a more negative range of potentials and reversed at more negative potentials, indicating a lower selectivity, than the main I_{Na} component. In this same preparation Ju *et al.* (1992) found that 100 nM TTX shortened the duration of the action potential with little effect on its amplitude, consistent with the findings of Coraboeuf *et al.* (1979). Sakakibara *et al.* (1992) working in human atrial cells found two classes of TTX binding sites. Ninety-two per cent of the total had a normal cardiac K_D of 1·3 μM and the remaining 8% had a K_D of 25 nM. Correspondingly, inactivation developed as the sum of two exponentials with the slower component constituting 8–9% of the total relaxation at potentials comparable to those at which TTX block was studied. At more negative potentials, the more slowly inactivating component constituted a larger fraction of the total suggesting that the channels generating this component activated over a more negative range of potentials. Certainly, the presence of two inactivation relaxations does not of itself indicate more than one channel type. However, the correspondence with the second class of TTX binding sites is suggestive of two populations of channels. The $I_{Ca(TTX)}$ reported in guinea-pig ventricular myocytes (Leblanc *et al.* 1996), human atrial cells (Lemaire *et al.* 1995) and rat ventricular myocytes (this study) provide additional evidence for more than one type of mammalian cardiac Na^+ channel.

With single-channel recording Cachelin *et al.* (1983) and Kunze *et al.* (1985) found a second, rare, type of Na^+ channel in rat ventricular myocytes distinguished by its lower conductance. In this same preparation Ju *et al.* (1994) found that late channel openings activated over a more negative range of potentials than did those appearing early in the step. The late opening channels had a longer mean open time, but in contrast to those of Cachelin *et al.* (1983) and Kunze *et al.* (1985) had about the same single channel conductance as the main, early opening type. A second, relatively rare, type of Na^+ channel with a lower single channel conductance than the main type has also been reported in canine cardiac Purkinje fibres (Scanley & Fozzard, 1987). Zilberter *et al.* (1994), working on rabbit Purkinje and ventricular cells, found that channels opening late during a depolarizing step had a shorter mean open time than those opening early. The shorter mean open time channels were more resistant to inactivation and constituted a larger fraction of the total at less depolarizing potentials, suggesting that they activated over a more negative potential range.

How many types of mammalian cardiac Na^+ channels are there?

Both an $I_{Ca(TTX)}$ and a second class of TTX binding sites have been reported in human atrial cells (Lemaire *et al.* 1995; Sakakibara *et al.* 1992), and both an $I_{Ca(TTX)}$ and an additional small I_{Na} component have also been described in rat ventricular myocytes (this study; Saint *et al.* 1992). If, in human atrial cells, the small, slower inactivating I_{Na} component does indeed arise from the small population of high affinity TTX binding sites, then $I_{Ca(TTX)}$ and the additional I_{Na} component in these cells both inactivate more slowly than the main body of classical Na^+ channels. And, in rat ventricular myocytes both $I_{Ca(TTX)}$ and the persistent I_{Na} component of Saint *et al.* (1992) activate over more negative potentials than the classical cardiac I_{Na}. However, in both of these cell types there are clear differences in the functional characteristics of $I_{Ca(TTX)}$ and the additional I_{Na} component.

The TTX IC_{50} for $I_{Ca(TTX)}$ in human atrial cells is about 1 μM (Lemaire *et al.* 1995). A similar value of 2·4 μM was reported for $I_{Ca(TTX)}$ in guinea-pig ventricular cells (Leblanc *et al.* 1996), and we find a K_D of 1·0 μM for $I_{Ca(TTX)}$ in rat ventricular myocytes. However, the second class of TTX binding sites in human atrial cells has a K_D of 25 nM (Sakakibara *et al.* 1992), and it is not possible to identify the channels generating the $I_{Ca(TTX)}$ in human atrial cells with those providing the second small class of TTX binding sites

owing to this fortyfold difference in reported TTX sensitivities. For rat ventricular myocytes, the separate nature of the channels generating the $I_{Ca(TTX)}$ and those responsible for the persistent I_{Na} can also be established.

We find an effective K_D for the TTX sensitivity of $I_{Ca(TTX)}$ in rat ventricular myocytes of 1·0 μM. However, Saint *et al.* (1992) found that 100 nM TTX blocked the persistent I_{Na} in rat ventricular myocytes nearly completely, suggesting a K_D for this persistent component in the nanomolar to tens of nanomolar range. It is not possible, then, to identify $I_{Ca(TTX)}$ channels with those generating the persistent current of Saint *et al.*

$I_{Ca(TTX)}$ channels, moreover, display no detectable persistent component, but, rather, seem to inactivate completely. Saint *et al.* (1992) found that the persistent I_{Na} was about 0·5% of the peak current in 2 mM Ca_o^{2+} and 130 mM Na_o^+. For the record of Fig. 12, peak current was −570 pA, and this peak decayed to a steady-state value not detectably different from zero. A steady-state inward current of as little as −10 pA or 1·75% of the peak would have been readily detectable (Fig. 12*B*). To attribute the persistent component to $I_{Ca(TTX)}$ channels, then, would require that $I_{Ca(TTX)}$ contributes nearly 30% of the total peak I_{Na} in 130 mM Na_o^+. However, it seems clear that $I_{Ca(TTX)}$ does not contribute this large a fraction of the total I_{Na} under these conditions. Brown *et al.* (1981) found two I_{Na} inactivation relaxations in rat ventricular myocytes, and their $\tau_{h,fast}(V)$ and $\tau_{h,slow}(V)$ values are consistent with our $\tau_{h,fast}(V)$ and $\tau_{h,slow}(V)$ data obtained in 1 mM Na_o^+ plus 0·5 mM Ca_o^{2+} (Fig. 10). Our $\tau_{h,slow}(V)$ component is generated by $I_{Ca(TTX)}$ channels, and it seems very likely, then, that the corresponding component of Brown *et al.* similarly arises from $I_{Ca(TTX)}$. Brown *et al.*, using considerably higher Na_o^+ concentrations than we did, found that 90% of the current decay could be accounted for by the faster inactivation process, and positive to −50 mV, $\tau_{h,fast}$ and τ_h obtained from a single-exponential fit were nearly identical. We obtained the same result under our experimental conditions. Both we and Brown *et al.* find that the slower inactivation relaxation contributes significantly to the single-exponential τ_h value only at more negative potentials, and we are now able to account for this voltage dependency of the relative contribution of the $\tau_{h,slow}$ component from the more negative range of activation of $I_{Ca(TTX)}$. At more positive potentials, however, where the classical cardiac Na^+ channels are also substantially activated, $I_{Ca(TTX)}$ channels weight the single-exponential τ_h negligibly and so contribute only a relatively small fraction of the total I_{Na}. Hence, if $I_{Ca(TTX)}$ channels generate the persistent I_{Na} component of Saint *et al.* (1992), they ought to display a persistent component which is more than a negligible fraction of the peak $I_{Ca(TTX)}$ and readily detectable in 5 mM Ca_o^{2+}, while none was seen experimentally, confirming that $I_{Ca(TTX)}$ channels are not the persistent Na^+ channels of Saint *et al.* Hence, the demonstration of the separate nature of $I_{Ca(TTX)}$ and the persistent component does not depend only on the different effective K_D values for TTX for these two components. Thus, rat ventricular myocytes express three functionally distinct types of Na^+ channels: the classical cardiac Na^+ channels, a population that is more TTX sensitive and generates a long-lasting I_{Na} component, and a population that is appreciably more Ca^{2+} permeable. Human atrial cells and possibly other mammalian cardiac cells as well similarly express three types of Na^+ channels.

If *heart I/SkM2* does indeed encode the main type of cardiac Na^+ channel, then the $I_{Ca(TTX)}$ channel is functionally distinct from both mammalian muscle Na^+ channel isoforms, SkM1 and SkM2. SkM2 channels inactivate more slowly, and activate and inactivate over more negative potential ranges than those encoded by *SkM1*, while the $I_{Ca(TTX)}$ channel inactivates yet more slowly and activates and inactivates over an even more negative potential range than the classical cardiac I_{Na}. It is not possible to identify $I_{Ca(TTX)}$ with SkM2 channels as SkM2 channels show no appreciable Ca^{2+} permeability (Pappone, 1980). While a single amino acid substitution can confer Ca^{2+} permeability on Na^+ channels (Heinemann, Terlau, Stühmer, Imoto & Numa, 1992), $I_{Ca(TTX)}$ channels differ from the other characterized I_{Na} components in cardiac cells by more than just permeability properties. Possibly the $I_{Ca(TTX)}$ channel corresponds to a differentially regulated, post-translationally modified or novel cardiac isoform. A novel Na^+ channel isoform, Na_v2, has in fact been identified in human cardiac and uterine tissue (George, Knittle & Tamkun, 1992) and a mouse atrial tumour cell line (Felipe, Knittle, Doyle & Tamkun, 1994). However, functional properties of the Na_v2 family are not known. Also, Sills *et al.* (1989) have identified a partial Na^+ channel sequence that appears to be specific for cardiac tissue and is distinct from both *SkM1* and *SkM2*.

The fact that $I_{Ca(TTX)}$ channels activate over a more negative range of potentials than the classical cardiac Na^+ channels suggests that they may play a critical role in depolarizing the membrane potential to action potential threshold. For example, from the Boltzmann fits of Fig. 7, at −55 mV, 15% of the $I_{Ca(TTX)}$ channels are activated while less than 0·1% of the other Na^+ channels are conducting. At −50 mV, 45% of the $I_{Ca(TTX)}$ but only 1% of the remaining Na^+ channels are activated. Hence, even though classical cardiac Na^+ channels must be substantially more frequent than $I_{Ca(TTX)}$ channels, there exists a range of potentials over which nearly all the g_{Na} activated is from $I_{Ca(TTX)}$ channels. These channels would be a major determinant in the triggering and conduction of the ventricular action potential. They should act to amplify the depolarization delivered to ventricular cells by Purkinje fibres and so serve to activate the main body of classical ventricular Na^+ channels. $I_{Ca(TTX)}$ channels may, therefore, be of particular importance for the problem of arrhythmias, and the gene encoding these channels could be a particularly effective target for gene therapy for cardiac arrhythmias.

AKAIKE, N. & TAKAHASHI, K. (1992). Tetrodotoxin-sensitive calcium-conducting channels in the rat hippocampal CA1 region. *Journal of Physiology* **450**, 529–546.

BAKER, P. F., HODGKIN, A. L. & RIDGEWAY, E. B. (1971). Depolarization and calcium entry in squid giant axons. *Journal of Physiology* **218**, 709–755.

BALKE, C. W. & WIER, W. G. (1992). Modulation of L-type calcium channels by sodium ions. *Proceedings of the National Academy of Sciences of the USA* **89**, 4417–4421.

BARRES, B. A., CHUN, L. L. Y. & COREY, D. P. (1989). Glial and neuronal forms of the voltage-dependent sodium channel: characteristics and cell-type distribution. *Neuron* **2**, 1375–1388.

BENOIT, E., CORBIER, A. & DUBOIS, J. M. (1985). Evidence for two transient sodium currents in the frog node of Ranvier. *Journal of Physiology* **361**, 339–360.

BOSSU, J. L. & FELTZ, A. (1984). Patch-clamp study of the tetrodotoxin-resistant sodium current in group C sensory neurons. *Neuroscience Letters* **51**, 241–246.

BROWN, A. M., LEE, K. S. & POWELL, T. (1981). Sodium current in single rat heart muscle cells. *Journal of Physiology* **318**, 479–500.

CACHELIN, A. B., DEPEYER, J. E., KOKUBUN, S. & REUTER, H. (1983). Sodium channels in cultured cardiac cells. *Journal of Physiology* **340**, 389–401.

CORABOEUF, E., DEROUBAIX, E. & COULOMBE, A. (1979). Effect of tetrodotoxin on action potentials of the conducting system in the dog heart. *American Journal of Physiology* **236**, H561–567.

FELIPE, A., KNITTLE, T. J., DOYLE, K. L. & TAMKUN, M. M. (1994). Primary structure and differential expression during development and pregnancy of a novel voltage-gated sodium channel in the mouse. *Journal of Biological Chemistry* **269**, 30125–30131.

FOX, A. P., NOWYCKY, M. C. & TSIEN, R. W. (1987). Kinetic and pharmacological properties distinguishing three types of calcium current in chick sensory neurons. *Journal of Physiology* **394**, 149–172.

GELLENS, M. E., GEORGE, A. L., CHEN, L., CHAHINE, M., HORN, R., BARCHI, R. L. & KALLEN, G. (1992). Primary structure and functional expression of the human cardiac tetrodotoxin-insensitive voltage-dependent sodium channel. *Proceedings of the National Academy of Sciences of the USA* **89**, 554–558.

GEORGE, A. L., KNITTLE, T. J. & TAMKUN, M. M. (1992). Molecular cloning of an atypical voltage-gated sodium channel expressed in human heart and uterus: Evidence for a distinct gene family. *Proceedings of the National Academy of Sciences of the USA* **89**, 4893–4897.

GILLY, W. F. & ARMSTRONG, C. M. (1984). Threshold channels – a novel type of sodium channel in squid giant axon. *Nature* **309**, 448–450.

GOLDMAN, L., AGGARWAL, R., SHOROFSKY, S. R. & BALKE, C. W. (1997). A new cardiac sodium current component in rat ventricular cells. *Biophysical Journal* **72**, A110.

GOLDMAN, L. & HAHIN, R. (1978). Initial conditions and the kinetics of the sodium conductance in *Myxicola* giant axons. II. Relaxation experiments. *Journal of General Physiology* **72**, 879–898.

GONOI, T., SHERMAN, S. J. & CATTERAL, W. A. (1985). Voltage clamp analysis of tetrodotoxin-sensitive and -insensitive sodium channels in rat muscle cells developing *in vitro*. *Journal of Neuroscience* **5**, 2559–2564.

HEINEMANN, S. H., TERLAU, W., STÜHMER, W., IMOTO, K. & NUMA, S. (1992). Calcium characteristics conferred on the sodium channel by single mutations. *Nature* **356**, 441–443.

HODGKIN, A. L. & KEYNES, R. D. (1957). Movement of labelled calcium in squid giant axons. *Journal of Physiology* **138**, 253–281.

JU, Y. K., SAINT, D. A. & GAGE, P. W. (1994). Inactivation-resistant channels underlying the persistent sodium current in rat ventricular myocytes. *Proceedings of the Royal Society of London* B **256**, 163–168.

KALLEN, R. G., SHENG, Z. H., YANG, J., CHEN, L., ROGART, R. B. & BARCHI, R. L. (1990). Primary structure and expression of a sodium channel characteristic of denervated and immature rat skeletal muscle. *Neuron* **4**, 233–242.

KIRSCH, G. E. & BROWN, A. M. (1989). Kinetic properties of single sodium channels in rat heart and rat brain. *Journal of General Physiology* **93**, 85–99.

KUNZE, D. L., LACERDA, A. E., WILSON, D. L. & BROWN, A. M. (1985). Cardiac Na currents and the inactivating, reopening, and waiting properties of single cardiac Na channels. *Journal of General Physiology* **86**, 691–719.

LEBLANC, N., CHARTIER, D., MARTIN, M. & COLE, W. C. (1996). Ca^{2+} permeation through Na^+ channels in guinea-pig ventricular myocytes. *Biophysical Journal* **70**, A279.

LEMAIRE, S., PIOT, C., SEGUIN, J., NARGEOT, J. & RICHARD, S. (1995). Tetrodotoxin-sensitive Ca^{2+} and Ba^{2+} currents in human atrial cells. *Receptors and Channels* **3**, 71–81.

MEVES, H. & VOGEL, W. (1973). Calcium inward currents in internally perfused giant axons. *Journal of Physiology* **235**, 225–265.

MITCHELL, M. R., POWELL, T., TERRAR, D. A. & TWIST, V. W. (1983). Characteristics of the second inward current in cells isolated from rat ventricular muscle. *Proceedings of the Royal Society* B **219**, 447–469.

OGATA, N. & TATEBAYASHI, H. (1992). Ontogenic development of the TTX-sensitive and TTX-insensitive Na^+ channels in neurons of the rat dorsal root ganglia. *Developmental Brain Research* **65**, 93–100.

PAPPONE, P. (1980). Voltage-clamp experiments in normal and denervated mammalian skeletal muscle fibres. *Journal of Physiology* **306**, 377–410.

PATLAK, J. B. & ORTIZ, M. (1985). Slow currents through single sodium channels of the adult rat heart. *Journal of General Physiology* **86**, 89–104.

ROGART, R. B., CRIBBS, L. L., MUGLIA, L. K., KEPHART, D. D. & KAISER, M. W. (1989). Molecular cloning of a putative tetrodotoxin-resistant rat heart Na^+ channel isoform. *Proceedings of the National Academy of Sciences of the USA* **86**, 8170–8174.

ROY, M. L. & NARAHASHI, T. (1992). Differential properties of tetrodotoxin-sensitive and tetrodotoxin-resistant sodium channels in rat dorsal root ganglian neurons. *Journal of Neuroscience* **12**, 2104–2111.

SAINT, D. A., JU, Y. K. & GAGE, P. W. (1992). A persistent sodium current in rat ventricular myocytes. *Journal of Physiology* **453**, 219–231.

SAKAKIBARA, Y., WASSERSTROM, J. A., FURUKAWA, T., JIA, H., ARENTZEN, C. E., HARTZ, R. S. & SINGER, D. H. (1992). Characterization of the sodium current in single human atrial myocytes. *Circulation Research* **71**, 535–546.

SCANLEY, B. E. & FOZZARD, H. A. (1987). Low conductance sodium channels in canine cardiac Purkinje cells. *Biophysical Journal* **52**, 489–495.

SILLS, M. N., XU, Y. C., BARACCHINI, E., GOODMAN, R. H., COOPERMAN, S. S., MANDEL, G. & CHIEN, K. R. (1989). Expression of diverse Na^+ channel messenger RNAs in rat myocardium. Evidence for a cardiac-specific Na^+ channel. *Journal of Clinical Investigation* **84**, 331–336.

TEN EICK, R., YEH, J. & MATSUKI, M. (1984). Two types of voltage dependent Na channels suggested by differential sensitivity of single channels to tetrodotoxin. *Biophysical Journal* **45**, 70–73.

THOMAS, G., BALKE, C. W. & SHOROFSKY, S. R. (1995). Calcium entry through sodium channels causes release of calcium from the sarcoplasmic reticulum in rat ventricular cells. *Biophysical Journal* **68**, A179.

WATANABE, A., TASAKI, I., SINGER, I. & LERMAN, L. (1967). Effects of tetrodotoxin on excitability of squid giant axons in sodium-free media. *Science* **155**, 95–97.

WEISS, R. E. & HORN, R. (1986). Functional differences between two classes of sodium channels in developing rat skeletal muscle. *Science* **233**, 361–364.

WEISS, R. E. & SIDELL, N. (1991). Sodium currents during differentiation in a human neuroblastoma cell line. *Journal of General Physiology* **97**, 521–539.

WENDT-GALLITELLI, M. F. & ISENBERG, G. (1985). Extra- and intracellular lanthanum: modified calcium distribution, inward currents and contractility in guinea pig ventricular preparations. *Pflügers Archiv* **405**, 310–322.

YAMAMOTO, D., YEH, J. Z. & NARAHASHI, T. (1984). Voltage-dependent calcium block of normal and tetramethrin-modified single sodium channel. *Biophysical Journal* **45**, 337–343.

ZILBERTER, Y. I., STARMER, C. F., STAROBIN, J. & GRANT, A. O. (1994). Late Na channels in cardiac cells: the physiological role of background Na channels. *Biophysical Journal* **67**, 153–160.

Acknowledgements

We thank Drs D. A. Hanck and W. G. Wier for critical reading of the manuscript, and Dr J. B. Patlak for stimulating discussions about these results. This work was supported by National Institutes of Health grants HL03542 to S.R.S. and C.W.B., HL02466 to C.W.B., HL50435 to C.W.B., a Veteran's Administration merit award to S.R.S. and C.W.B., a grant-in-aid from the American Heart Association (Maryland Affiliate) to C.W.B., a grant-in-aid from the American Heart Association (Maryland Affiliate) to S.R.S. and a grant-in-aid from the National American Heart Association to L.G.

Author's email address

C. W. Balke: bbalke@heart.ab.umd.edu

Received 19 May 1997; accepted 11 August 1997.